Physica C 190 (1992) 299–303
North-Holland

PHYSICA C

Electron–phonon coupling in $Ba_{0.6}K_{0.4}BiO_3$ by discretized quantum path integral molecular dynamics

C.Y. Lee [a] and P.A. Deymier [b]

[a] *Department of Physics, University of Arizona, Tucson, AZ 85721, USA*
[b] *Department of Materials Science and Engineering, University of Arizona, Tucson, AZ 85721, USA*

Received 17 September 1991

We calculated the electron–phonon interaction energy and estimated the electron–phonon coupling constant in $Ba_{0.6}K_{0.4}BiO_3$ using a quantum path integral molecular dynamics. We determined the electron–phonon coupling constant at room temperature to be about 1.34.

1. Introduction

The discovery by Müller and Bednorz of superconductivity in copper oxides [1], has led to a great deal of research to understand the physical origin of the high temperature superconductivity. More recently copper free oxide superconductors such as potassium doped $BaBiO_3$ have shown high T_c (~ 30 K) [2,3]. Compared to copper oxide $Ba_{1-x}K_xBiO_3$ is a structurally and electronically simple system. A clear isotope effect for oxygen replacement with $\alpha \simeq 0.4$ for the bismate superconductor was measured by Hinks et al. [4]. A photon softening between $BaBiO_3$ and $Ba_{0.6}K_{0.4}BiO_3$ was described by Loong et al. [5]. These experimental evidences support driven mechanism for superconductivity in this material [6,7]. Previous experimental data by Kondoh et al. [8] also showed that this material involves a weak to moderate electron–phonon coupling as measured by the coupling constant, $\lambda \simeq 1$ near T_c. In this paper, we employ for the first time the computational method of discretized quantum path integral molecular dynamics to estimate the electron–phonon coupling constant in $Ba_{0.6}K_{0.4}BiO_3$.

2. Computational method and model

A theoretical approach to the problem of the electron–phonon interaction in the high-T_c oxide materials presents great difficulties since quantum mechanics and statistical physics are interwoven in a complicated way. A discretized version of Feynman's path integral formulation of quantum statistical mechanics [9] makes possible the simulation of quantum many-body systems. This method may provide a convenient framework for shedding light on the problem of the interaction between a conduction electron and an oxide lattice.

Within a high temperature approximation, the quantum partition function of a quantum particle in some external potential $\phi(r)$ can be shown to take the form of a classical partition function [10].

$$Z \simeq Z_p = \left(\frac{pm}{2\pi\hbar^2\beta^2}\right)^{3p/2} \int dr_1 dr_2 dr_3 \ldots dr_p \times \exp(-\beta V_{\text{eff}}(r_1 \ldots r_p)) , \quad (1)$$

with

$$V_{\text{eff}}(r_1 \ldots r_p) = \sum_{i=1}^{p} \left[\left(\frac{pm}{2\hbar^2\beta^2}\right)(r_i - r_{i+1})^2 + \frac{1}{p}\phi(r_i) \right].$$

where p represents a number of intermediate configurational states forming a loop closing in on state r_1. In the summation over the p states, it is understood that $r_{p+1} = r_1$. The quantum particle may therefore be represented by a necklace of p nodes such that

a point on the necklace interacts with its first neighbors in the chain through a harmonic potential of spring constant $pm/\hbar^2\beta^2$. The isomorphism between quantum and classical representations becomes more accurate as $p\to\infty$. The total effective potential energy of a crystal containing a single electron is given by

$$V_{\text{eff}}=\sum_{i=1}^{p}\frac{pm}{2\hbar^2\beta^2}(r_i-r_{i+1})^2+\frac{1}{p}\sum_{i=1}^{p}\sum_{J=1}^{p}\phi_{eJ}(r_i-R_J)+\tfrac{1}{2}\sum_{I=1}^{N}\sum_{J=1}^{N}\phi_{IJ}(R_I-R_J)\,, \qquad (2)$$

where the R_{IJ} are the ionic coordinates, r_i is the electron coordinate, and ϕ_{eJ} and ϕ_{IJ} are the electron–ion and ion–ion interaction potentials. A classical molecular dynamics (MD) method can then be employed to sample the system phase space. For this we use a MD algorithm similar to the one described in details by Parrinello and Rahman (P&R) [10]. The cation–electron interactions are modelled with a pseudopotential. The core radius of K is taken at 1.96 Å in reference to the work of P&R [10], the core radius of Ba is arbitrarily taken at 1.96 Å. The core radius for Bi is varied between 1.5 and 1.75 Å. 1.5 Å corresponds to a deep potential well. Over 1.75 Å the cores of neighboring cations overlap. We vary the Bi core to scan the electronic band structure from low energy levels up to electronic conductive behavior near Bi core overlap. Although the oxygen core radius exists in nature, we neglect the core corrections for oxygen because of the long range repulsive coulombic interaction between the electron and O^{2-}. We employ a classical ionic model for the $Ba_{0.6}K_{0.4}BiO_3$ lattice. Details of this model are reported elsewhere [11].

The system is simulated with a constant temperature, $T=300$ K, and pressure, $P=1$ atm. The time integration step is 2.68×10^{-15} s. The question of convergence of the properties of the quantum particle as a function of P was addressed. We tested a sequence of numbers of necklace nodes. We has almost consistent results and satisfactory convergence of the isomorphism at $T=300$ K for $P\geq400$. This result is similar to the findings of Landman et al. [12] in their study of an electron in a KCl crystal at room temperature.

We begin the computer simulations by running 5000 time steps for equilibration of the ionic lattice. After that period, a 400 particle necklace was inserted within the core of a prescribed bismuth ion. When we inserted the quantum system, we also subtracted equivalent charges from each of the 64 individual Bi ions to ensure charge neutrality in the whole system. Simulations were run for a period of 5000 steps to equilibrate the quantum system. All average properties are then calculated over a period of 3000 steps.

In the discretized path integral MD described here, the equilibrium state of the electron results from a self-consistent mutual interaction between the p nodes and the ionic species. In this case, the ions are allowed to displace to accommodate the electron, the electron in turn responds to these displacements. The electron energy calculated with this method includes a contribution from the electron–phonon interaction.

If we eliminate from the algorithm all effects of forces the electron nodes apply on the ions while maintaining the electrostatic forces on the electron due to the ions, one excludes the electron–phonon interaction from the electron energy. In this case, only thermal effects resulting from phonon interaction with the electron are accounted for.

We call type1 simulation the complete path integral molecular dynamics and type0 the artificially altered algorithm. The electron–phonon coupling energy is calculated as the difference between the equilibrium electron potential energy in type1 and type0 simulations.

3. Results and discussion

In fig. 1 we report the electron–cation, electron–anion correlation function for two extreme values of the Bi core radius. The location of the correlation peaks in type1 and type0 shows that the cations do not displace significantly in response to the incoming electron. Part of the reason may be that the electron density is spherically symmetric centered on the Bi ion thus not perturbating its position. The electron–cation correlation, as well as the difference in correlation between type1 and type0 simulations, is drastically reduced from $R=1.5$ Å to $R=1.75$ Å. For $R=1.5$ Å, the electron is strongly correlated to the cations. This behavior is characteristic of a localized

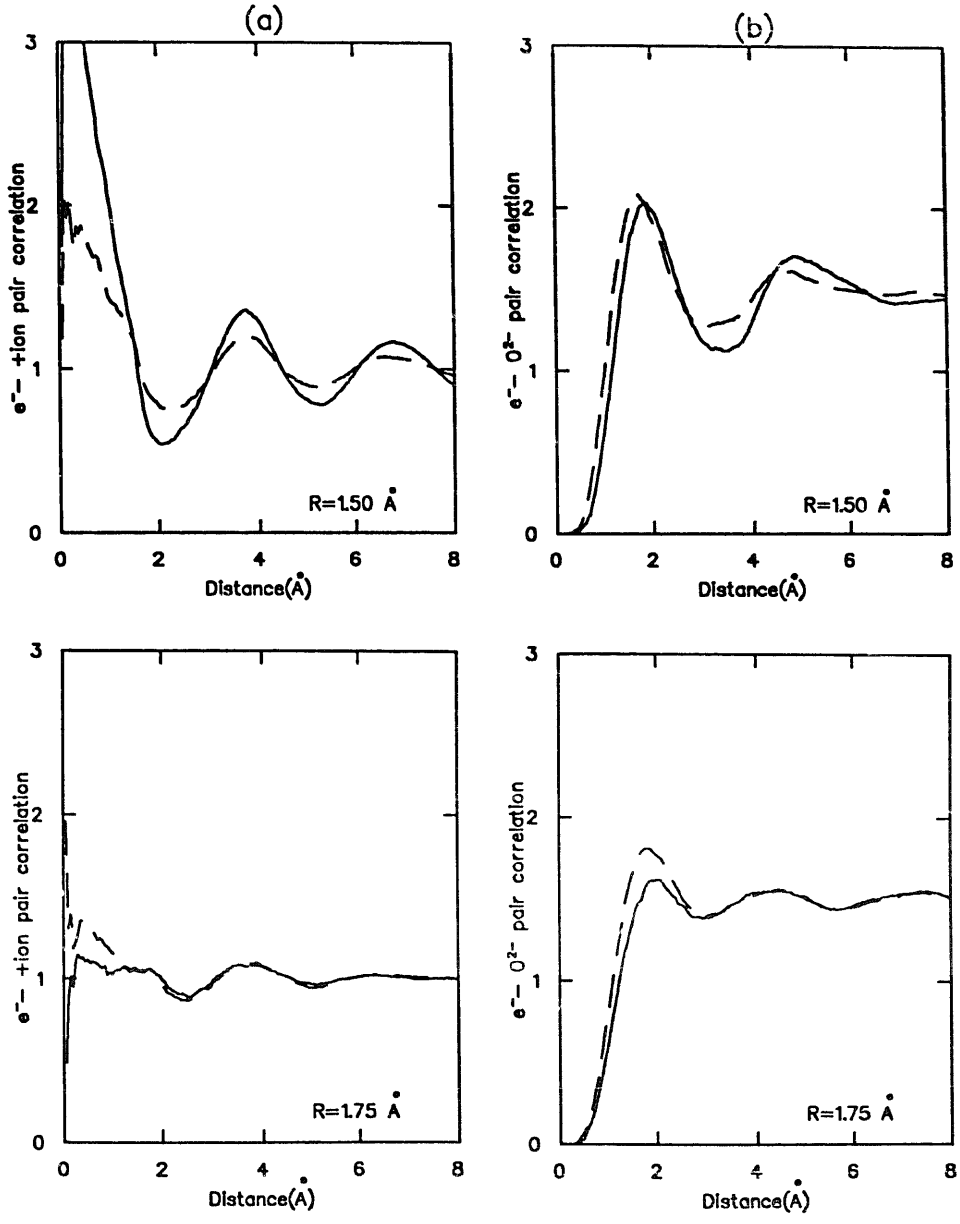

Fig. 1. (a) Electron–cation radial correlation; (b) Electron–anion radial correlation (–) and (...) stand for simulations of type1 and type0 (see text for details).

electron within the Bi core. In the case of the larger value of the Bi core ($R=1.75$ Å), the electron–cation correlation is reduced as indicated by the almost uniform distribution in both type1 and type0 simulations. This electron mimics the behavior of a conduction electron.

We also present the electron–oxygen correlations for various Bi core radii. For small core radius $R=1.5$ Å, the electron is well localized inside the Bi core. This localization is also apparent in the sharpness of the electron–oxygen correlation peak. In contrast, as the Bi core increases to $R=1.75$ Å, broader peaks in the electron–oxygen correlation appear, a sign of electron delocalization. Furthermore, at $R=1.5$ Å, a significant difference in location of the first peak in the electron–oxygen correlation between type1 and type0 simulations can be noted. This difference of approximately 0.2 Å represents the oxygen relaxa-

Table 1
Electron potential energy, PE, in eV (a) with e^--ph interaction (type1 simulations), (b) without e^--ph interaction (type0 simulations) and e^--ph interaction, ΔE, vs. Bi core radius, R. The σ are the uncertainties on the calculated energies

R (Å)	(a) PE(σ)	(b) PE(σ)	$\Delta E(\sigma)$
1.50	−16.459(0.028)	−8.265(0.028)	−8.194(0.057)
1.55	−12.153(0.001)	−7.300(0.043)	−4.853(0.057)
1.60	−8.352(0.001)	−6.393(0.001)	−1.959(0.028)
1.65	−5.860(0.100)	−5.443(0.01)	−0.302(0.100)
1.75	−4.766(0.001)	−4.608(0.024)	−0.150(0.028)

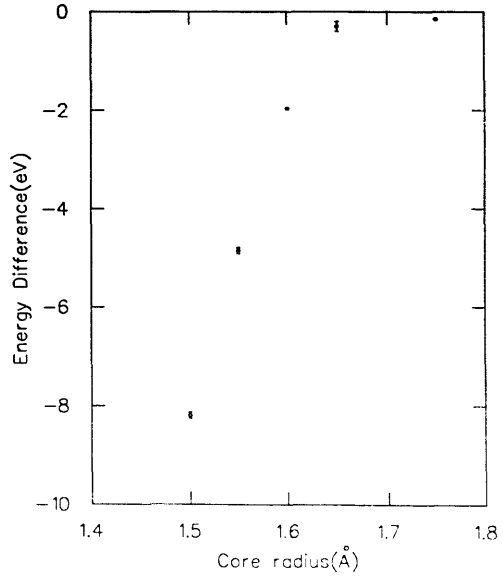

Fig. 2. Electron-phonon interaction energy vs. Bi core radius.

tion due to the presence of the electron. For larger cores, such as $R=1.75$ Å, a smaller (0.125 Å) difference in the first electron-oxygen correlation peak can be detected indicating a weaker interaction between the electron and the oxygen ions (note that the resolution limit on the calculation of the correlation function is 0.05 Å). In table 1 and fig. 2, we report and plot the electron-phonon coupling energy for various values of the Bi core radius. The coupling energy drastically decreases in the interval $R\in[1.5\text{–}1.6]$. This large variation results from the reduction in electron-cation correlation. In the range $R\in[1.5\text{–}1.6]$, the energy is converging to a value of approximately 0.15 eV. This value is characteristic of the electron-oxygen phonon interaction.

To estimate the electron-phonon coupling constant, we take the simulation $R=1.75$ Å as being representative of an electron-oxygen sublattice interaction in $Ba_{0.6}K_{0.4}BiO_3$. We use the potential energy difference, $\Delta E=0.15$ eV, at $R=1.75$ Å with the relation, $\lambda=\Delta E/\hbar\omega_L$, where ω_L is the optical longitudinal phonon frequency. In ref. [11] it was found that the high energy vibrational modes within the classical ionic model of $Ba_{0.6}K_{0.4}BiO_3$ are associated with oxygen vibrations. The oxygen ion exhibits vibrational modes at about 610 cm^{-1} and about 800 cm^{-1} parallel to the Bi–O bond while modes of vibration perpendicular to the Bi–O bond cover a wide interval of frequencies from 150 to 600 cm^{-1}. A lower limit for the coupling constant is obtained by choosing the longitudinal phonon frequency ω_L at the oxygen frequency of 800 cm^{-1}. The corresponding value of the coupling constant is about 1.18. For an upper bound of the coupling constant, we choose the oxygen frequency at about 600 cm^{-1} which corresponds to the lowest frequency for the Bi–O stretching mode. The corresponding value for the maximum coupling constant is 1.57. We estimate an average value for the coupling constant of about 1.34. This value is within the range of weak to intermediate electron-phonon coupling.

References

[1] J.G. Bednorz and K.A. Müller, Z. Phys. B 64 (1986) 189.
[2] L.F. Mattheiss, E.M. Gyorgy and D.W. Johnson Jr., Phys. Rev. B 37 (1988) 3745.
[3] D.G. Hinks, D.R. Richards, B. Dabrowski, D.T. Marx and A.W. Mitchell, Nature (London) 335 (1988) 419.
[4] D.G. Hinks, B. Dabrowski, J.D. Jorgensen, A.W. Mitchell, D.R. Richards, S. Pei and D. Shi, Nature (London) 333 (1988) 836.

[5] C.K. Loong, P. Vashishta, R.K. Kalia, M.H. Degani, D.L. Price, J.D. Jorgensen, D.G. Hinks, B. Dabrowksi, A.W. Mitchell, D.R. Richards and Y. Zheng, Phys. Rev. Lett 62 (1989) 2628.
[6] K.F. McCarthy, H.B. Radousky, D.G. Hinks, Y. Zheng, A.W. Mitchell, T.J. Folkerts and R.N. Shelton, Phys. Rev. B 40 (1989) 2662.
[7] B. Batlogg, R.J. Cava, L.W. Rupp Jr., A.M. Mujsce, J.J. Krajewski, J.P. Remeika, W.F. Peck Jr., A.S. Cooper and G.P. Espinosa, Phys. Rev. Lett. 61 (1988) 1670.
[8] S. Kondoh, M. Sera, Y. Ando and M. Sato, Physica C 157 (1989) 469.
[9] R.P. Feynman and A.R. Hibbs, Quantum Mechanics and Path Integrals (McGraw-Hill, New York, 1965).
[10] M. Parrinello and A. Rahman, J. Chem. Phys. 80 (1984) 860.
[11] C.Y. Lee and P.A. Deymier, Physica B 168 (1991) 268.
[12] U. Landman, D. Scharf and J. Jortner, Phys. Rev. Lett. 54 (1985) 1860.